Electrogenerated chemiluminescence of benzo 15-crown-5 derivatives

Xiao Jiang[a], Xichuan Yang[a]*, Changzhi Zhao[b] and Licheng Sun[a,c]

Novel electrogenerated chemiluminescence (ECL) reagents C1, C2, and C3 with high fluorescence quantum yields bearing 15-crown-5 moiety have been synthesized and characterized. The photophysical, electrochemical, and ECL characters of these compounds have been studied in a 1:1 (v/v) PhH/MeCN mixed solvent. The ECL intensity is enhanced distinctly with the increase in the fluorescence quantum yield. Their ECL behaviors have been studied using annihilation and co-reactant methods (tri-*n*-propylamine (TPrA) was used as a co-reactant), respectively. The stable ECL emissions of compounds C1–C3 can be ascribed to the typical and simple monomer ECL emission via S-route. Copyright © 2008 John Wiley & Sons, Ltd.

Supporting information may be found in the online version of this article.

Keywords: Electrogenerated Chemiluminescence (ECL), 15-Crown-5 derivatives, Annihilation ECL, Co-reactant ECL

INTRODUCTION

Since the first detailed studies in the mid-1960s electrogenerated chemiluminescence (ECL) has attracted much attention and been studied extensively. It provides a powerful tool for understanding fundamental questions in analytical chemistry, biology, and physics. During the past two decades, numerous studies on the ECL of inorganic complexes and/or clusters have been reported, in particular $Ru(bpy)_3^{2+}$ and its derivatives which play a pivotal role in transforming ECL from a laboratory curiosity to a useful, and commercially viable, analytical technique.[1–10] In addition, organic systems capable of generating ECL, such as polymers, fluorescent laser dyes, polyaromatic hydrocarbons (PAHs), and donor–acceptor functionalized compounds, are also of interest.[11–21] There are several general criteria for organic materials to be suitable for ECL: high fluorescence quantum yield, the electrochemical stability, and the high efficiency of electron- and energy-transfer. Additionally, its ability to produce ECL under moderate conditions in aqueous buffered solutions will be extremely important in practical applications. Accordingly our work focuses on those molecules which not only are efficient in generating ECL, but also have moderate water solubility.

It is well known that many organic molecules with crown ether moiety or analogous heteroatom crown ether unit have been employed to detect the metal ions as highly sensitive fluorescent chemosensors.[22–24] Considering the potential applications of the compounds containing crown ether moiety for detection of metal ions under ECL conditions,[25,26] we designed a series of new functional organic molecules C1–C3 with 15-crown-5 moiety (a double armed unit is bound to the crown ether in the 2,3-positions) shown in Chart 1. Here we mainly report the synthesis and their ECL behaviors in organic solvent and the possible mechanisms.

RESULTS AND DISCUSSION

### Synthesis and characterization

Compounds **C1**–**C3** were prepared according to a general synthetic procedure shown in Scheme 1. Diethylene glycol as the starting material reacted with *p*-toluenesulfonyl chloride to give compound **1**.[27] Compound **1** was treated by catechol in the presence of Bu$_4$NI to afford compound **2**.[28] Reaction of **2** with a solution of HBr in acetic acid and paraformaldehyde led to the intermediate **3**, which directly reacted without purification with triethyl phosphite to get the precursor **4**.[29] Similarly, compound **4** was also directly used without further purification in the next synthesis step. The target compound **C1** was prepared by Witting–Horner reaction of **4** with 4-*N*,*N*-dimethylamino-benzaldehyde in the presence of NaH.[30,31] Compounds **C2** and **C3** were obtained by a similar procedure to **C1**. All

*   *Correspondence to: X. Yang, State Key Laboratory of Fine Chemicals, DUT-KTH Joint Education and Research Center on Molecular Devices, Dalian University of Technology (DUT), 158 Zhongshan Road, 116012 Dalian, PR China. E-mail: yangxc@dlut.edu.cn*

a   *X. Jiang, X. Yang, L. Sun*
State Key Laboratory of Fine Chemicals, DUT-KTH Joint Education and Research Center on Molecular Devices, Dalian University of Technology (DUT), 158 Zhongshan Road, 116012 Dalian, PR China

b   *C. Zhao*
College of Chemistry and Molecular Engineering, Qingdao University of Science and Technology, 53 Zhengzhou Road, 266042 Qingdao, PR China

c   *L. Sun*
KTH School of Chemical Science and Engineering, Organic Chemistry, Royal Institute of Technology (KTH), Teknikringen 30, 10044 Stockholm, Sweden
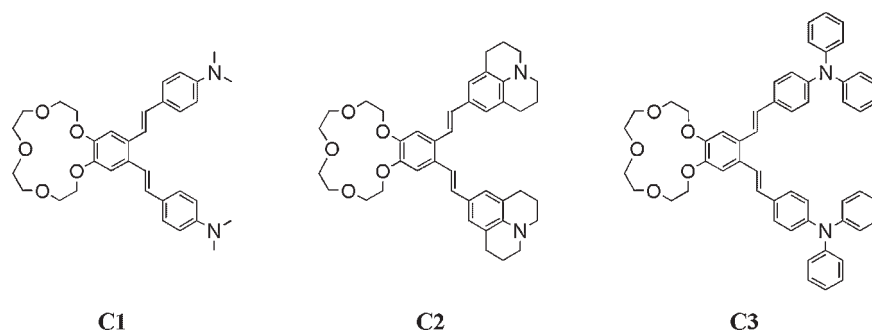
Chart 1. Structures of compounds **C1**–**C3**

Table 1. Photophysical, electrochemical,[a] and ECL characters of compounds **C1**–**C3** in 1:1 PhH/MeCN

Compound	λ_{abs} (nm)[b]	λ_{em} (nm)	Φ_{em}[c]	E_g (eV)[d]	$E_{pa}(1)$ (V)	$E_{pa}(2)$ (V)	E_{pc} (V)	E_{HOMO} (eV)[e]	E_{LUMO} (eV)[f]	λ_{ECL} (nm)	E_s (eV)[g]	$-\Delta H^\circ$ (eV)
C1	343 (377)	483	0.166	2.86	0.29	0.42	−2.45	−4.90	−2.04	493	2.57	2.64
C2	364 (392)	504	0.253	2.74	0.24	0.58	−2.49	−4.88	−2.14	505	2.46	2.63
C3	359 (390)	479	0.487	2.81	0.68	0.99	−2.33	−5.33	−2.52	483	2.59	2.91

[a] *Versus* SCE.
[b] The shoulder peak is given in parentheses.
[c] Fluorescence quantum yield (Φ_{em}) were measured in MeCN with reference to quinine sulfate ($\Phi_{em} = 0.508$ in 0.05 M H_2SO_4).[32]
[d] Calculated from λ_{onset} in absorption spectrum.
[e] $E_{HOMO}/eV = -4.74/eV - eE_{onset}^{ox}$.[33]
[f] $E_{LUMO}/eV = E_g + E_{HOMO}$.
[g] Calculated from the highest energy emission peak in fluorescence spectrum.

compounds were characterized by ^{1}H NMR, ^{13}C NMR, and HRMS.

Photophysical properties

The photophysical data of compounds **C1**–**C3** in 1:1 PhH/MeCN solution at a concentration of 1×10^{-5} M are listed in Table 1. Figure 1 displays the absorption spectra of compounds **C1**–**C3**. It can be observed that each compound shows an absorption peak in the higher energy region and a shoulder in the lower energy region, which can be attributed to the absorption of the single-armed unit and the whole molecule, respectively. According to literature, the *N,N*-diaryl-substituted stilbene derivatives have inherently greater fluorescence quantum yields (Φ_{em}) and longer lifetimes due to the prominent "amino conjugation effect," as compared with the *N,N*-dialkyl-substituted stilbene derivatives.[34] Therefore, we can see from Table 1 that the Φ_{em} of **C3** is close to 0.5, which is obviously larger than that of **C1** and **C2**. Furthermore, the high fluorescence quantum efficiency is advantageous for ECL which will be discussed below.

Electrochemical analysis

The redox potentials of compounds **C1**–**C3** in 1:1 PhH/MeCN solution at a concentration of 1×10^{-3} M are listed in Table 1. Cyclic voltammogram (CV) of compound **C3** is shown in Fig. 2.

Due to the limitation of the potential window of the solvent, the cathodic reduction wave of compound **C3** is not well resolved, a differential pulse voltammogram (DPV) displays that it has clear cathodic reduction, which is shown in inset of Fig. 2. On the
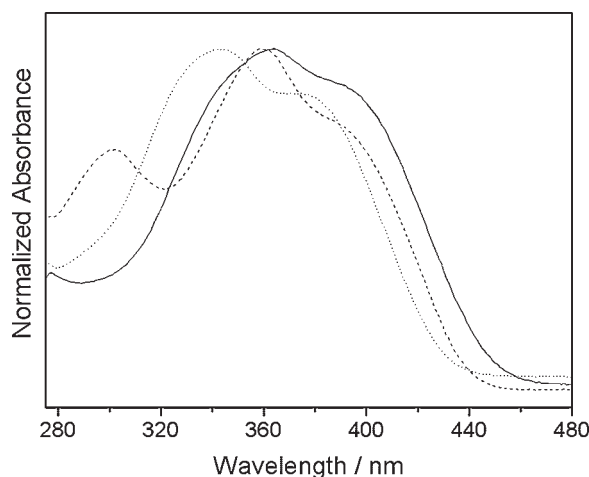

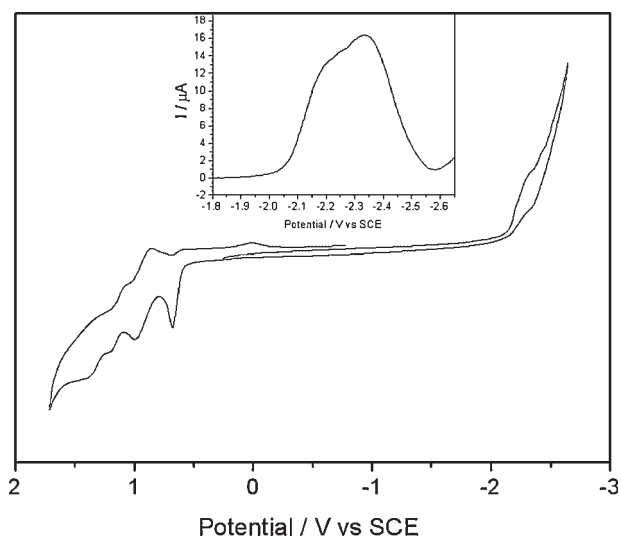**Figure 1.** Normalized absorption spectra of **C1** (dot), **C2** (solid), and **C3** (dash) in 1:1 PhH/MeCN

Figure 2. CV of **C3** with 0.05 M TBAPF$_6$ as a supporting electrolyte in 1:1 PhH/MeCN using a platinum working electrode and an Ag/Ag$^+$ reference electrode, scan rate 100 mV s^{-1}. Inset: DPV of **C3**

Figure 4. ECL (1×10^{-3} M, solid) and fluorescence (1×10^{-5} M, dash) spectra of **C3** in 1:1 PhH/MeCN

oxidation side, the first wave at $+0.68$ V (*vs*. SCE) is ascribed to the oxidation of one of substituted amino groups, and the second wave at $+0.99$ V (*vs*. SCE) is assigned to the oxidation of the other substituted amino group. On the reduction side, the irreversible wave at -2.33 V (*vs*. SCE) is ascribed to the reduction of the crown ether moiety. It is also observed that the presence of triphenylamine unit in the backbone decreases the highest occupied molecular orbital (HOMO) and the lowest unoccupied molecular orbital (LUMO) energy levels of compound **C3** compared with the other two compounds **C1** and **C2**.

Electrogenerated chemiluminescence (ECL) in nonaqueous system

Annihilation ECL and co-reactant ECL are two of general ECL reaction mechanisms. Annihilation ECL involved electron-transfer
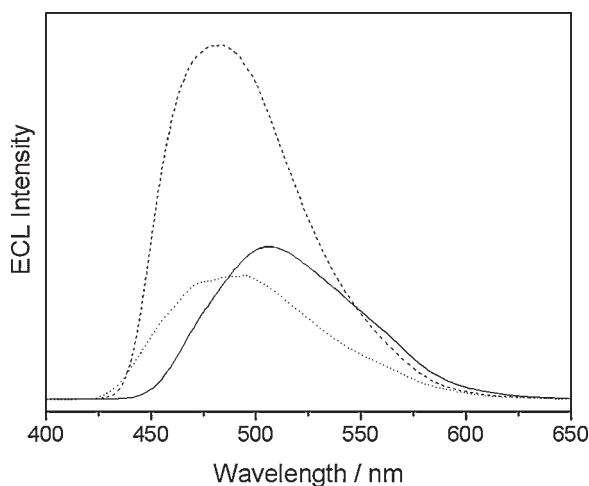
reactions between an oxidized and a reduced species, both of which were generated at an electrode by alternate pulsing of the electrode potential. This approach is a typical double-potential step.[1] It is also possible to generate ECL in a single-potential step using a co-reactant. A co-reactant is a species that, upon oxidation or reduction, produces an intermediate that can react with an ECL luminophore to produce excited states. In an ECL system, addition of a co-reactant assisting to generate ECL is fairly common, such as tri-*n*-propylamine (TPrA), which is an especially important "oxidative–reductive" co-reactant for practical applications because it allows efficient ECL not only in aqueous media but also at physiological pH ($\sim$7.4).[1–5] In this section, the ECL behaviors of compounds **C1**–**C3** will be discussed using annihilation and co-reactant methods in nonaqueous system (1:1 PhH/MeCN), respectively.

Figure 3. ECL spectra of **C1** (dot), **C2** (solid), and **C3** (dash) with a sample concentration of 1×10^{-3} M in 1:1 PhH/MeCN containing 0.05 M TBAPF$_6$ as a supporting electrolyte. The potential was stepped from -2.7 V to $+1.0$ V, pulsed for 0.5 s
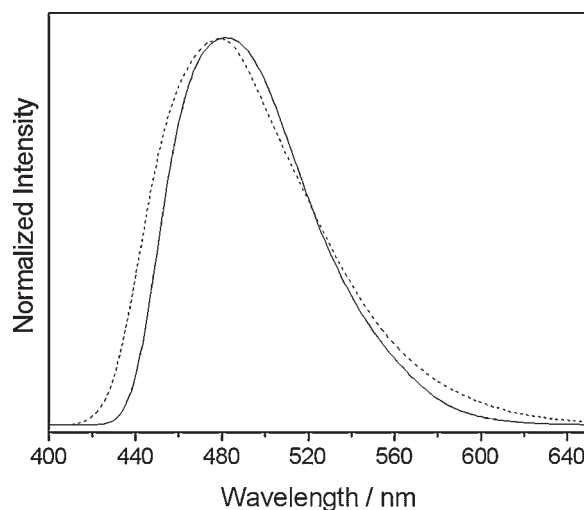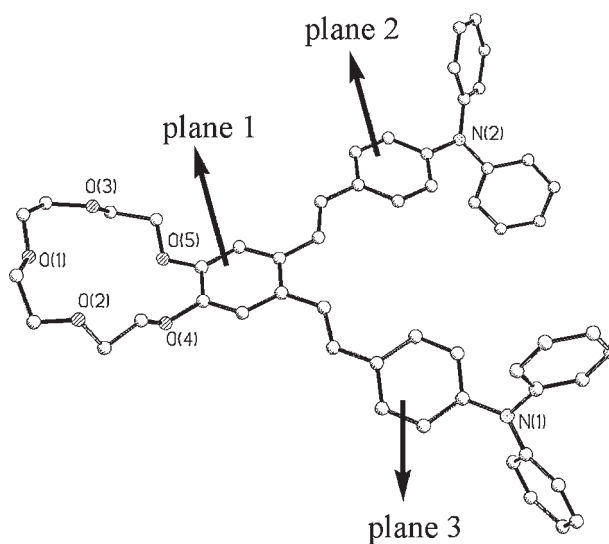

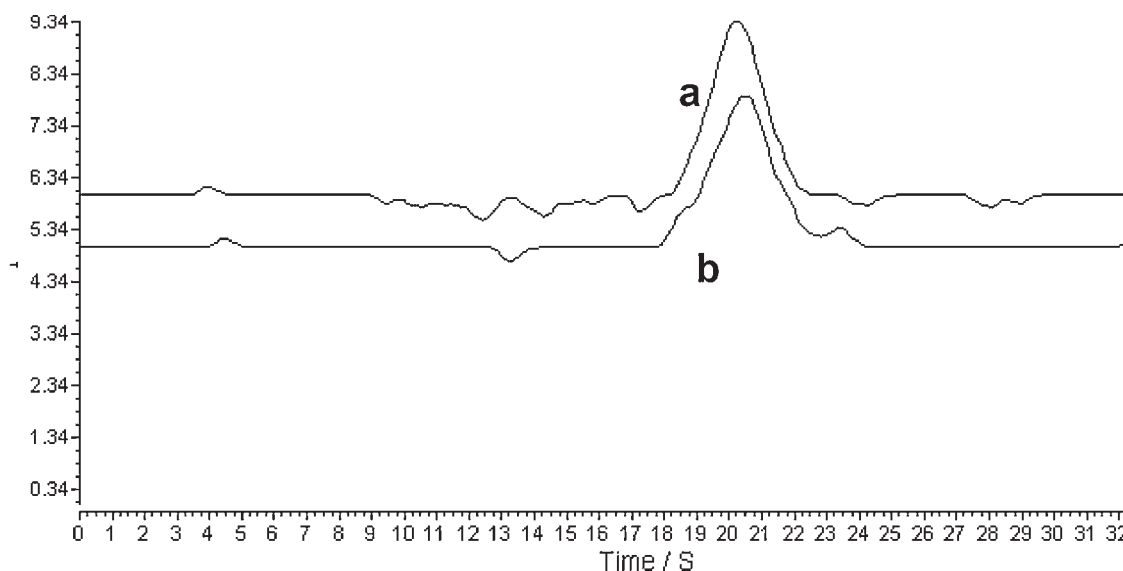**Figure 5.** X-ray crystal structure of compound **C3**

Figure 6. Time-intensity ECL spectra of (a) 1×10^{-5} M and (b) 1×10^{-3} M solutions of **C3** in 1:1 PhH/MeCN containing 0.05 M TBAPF$_6$ as a supporting electrolyte. The potential was stepped from 2.7 to $+1.0$ V
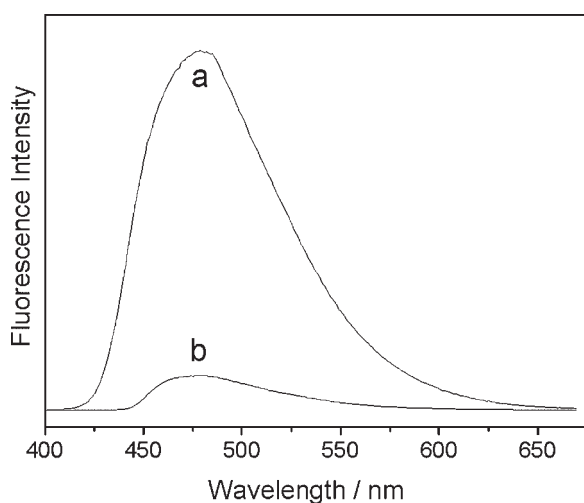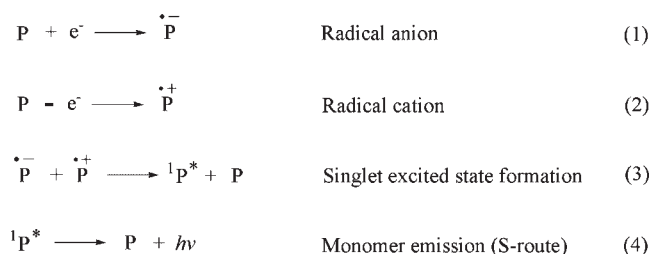

Figure 7. Fluorescence spectra of compound **C3** (a) 1×10^{-5} M, (b) 1×10^{-3} M in 1:1 PhH/MeCN

Annihilation ECL

ECL spectra are recorded at room temperature using a setup consisting of a fluorescence spectrophotometer and a cyclic voltammograph with a computer interface.[35] Measurements are obtained in the same concentration (1×10^{-3} M) as used for the CV. The ECL data of all compounds are summarized in Table 1. Figure 3 shows the ECL spectra of compounds **C1**–**C3** under the same experimental conditions. It is found that there is a good correlation between the observed ECL intensity and Φ_{em}. The ECL intensities of **C1**–**C3** are enhanced greatly with the increases in

reaction sequence 1

$$P \;-\; e^- \longrightarrow \overset{\bullet +}{P} \tag{5}$$

$$Pr_2NCH_2CH_2CH_3 \;-\; e^- \longrightarrow Pr_2NCH_2CH_2CH_3^{\bullet +} \tag{6}$$

$$Pr_2NCH_2CH_2CH_3^{\bullet +} \longrightarrow Pr_2N\overset{\bullet}{C}HCH_2CH_3 \;+\; H^+ \tag{7}$$

$$\overset{\bullet +}{P} \;+\; Pr_2N\overset{\bullet}{C}HCH_2CH_3 \longrightarrow {}^1P^* \;+\; Pr_2\overset{+}{N}CH_2CH_2CH_3 \tag{8}$$

$${}^1P^* \longrightarrow P \;+\; h\nu \tag{9}$$

or reactions 5-7 are then followed by

reaction sequence 2

$$P \;+\; Pr_2N\overset{\bullet}{C}HCH_2CH_3 \longrightarrow \overset{\bullet -}{P} \;+\; Pr_2\overset{+}{N}CH_2CH_2CH_3 \tag{10}$$

$$\overset{\bullet -}{P} \;+\; \overset{\bullet +}{P} \longrightarrow {}^1P^* \;+\; P \tag{11}$$

$${}^1P^* \longrightarrow P \;+\; h\nu \tag{12}$$

P represents compound **C1** or **C2** or **C3**

Scheme 3. Proposed mechanisms for co-reactant ECL of compounds **C1**–**C3**

$$P \;+\; e^- \longrightarrow \overset{\bullet -}{P} \qquad \text{Radical anion} \tag{1}$$

$$P \;-\; e^- \longrightarrow \overset{\bullet +}{P} \qquad \text{Radical cation} \tag{2}$$

$$\overset{\bullet -}{P} \;+\; \overset{\bullet +}{P} \longrightarrow {}^1P^* + P \qquad \text{Singlet excited state formation} \tag{3}$$

$${}^1P^* \longrightarrow P \;+\; h\nu \qquad \text{Monomer emission (S-route)} \tag{4}$$
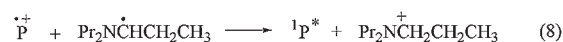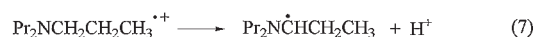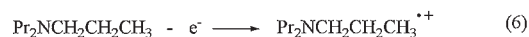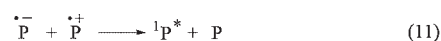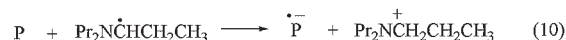
P represents compound **C1** or **C2** or **C3**

Scheme 2. Proposed mechanism for annihilation ECL of compounds **C1**–**C3**

4
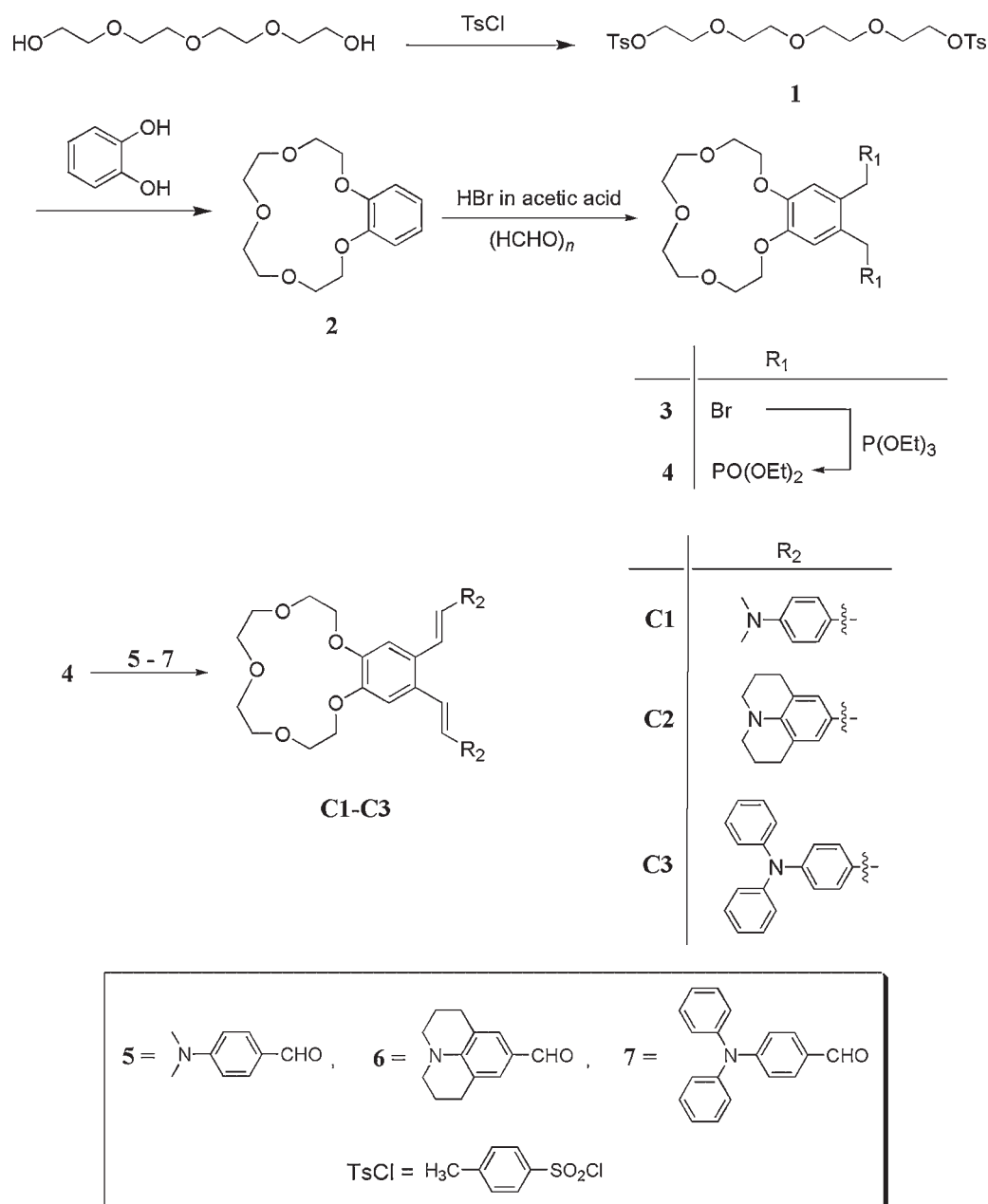
Scheme 1. Synthesis of compounds **C1**–**C3**

their Φ_{em}. Thus those compounds with high Φ_{em} are more suitable for ECL. Figure 4 exhibits the ECL and fluorescence spectra of compound **C3**. As illustrated in Fig. 4, the ECL emission curve and bandwidth of **C3** are similar to those of fluorescence, and the ECL maximum (λ_{ECL}) are in good match with its fluorescence maximum (λ_{em}) with slight red shift (only 4 nm), indicating the formation of the same excited state in both experiments.

The X-ray crystal structure of compound **C3** (Fig. 5) shows that the molecule has a completely nonplanar structure.[36] The crown ether ring shows a zigzag conformation and the structure of triphenylamine group looks like a windstick. The two bridge units linked by double bond between crown ether ring and substituted amino group are also torsional (the dihedral angle between planes 1 and 2 is 14.4°, and that between planes 1 and 3 is 22.7°).

In addition, there is no observable increase in ECL intensity of compound **C3** when the sample concentration is enhanced from 1×10^{-5} to 1×10^{-3} M (Fig. 6).

Figure 7 shows the fluorescence spectra of **C3** with different concentrations in 1:1 PhH/MeCN mixed solvent excited at 360 nm. The monomer fluorescence emission intensity at *ca.* 480 nm is decreased dramatically with increasing the sample concentration from 1×10^{-5} to 1×10^{-3} M. However, no any new emission band is observed in the longer or shorter wavelength region.

As a result, on the basis of our previous studies,[13,14] the possibility of excimer or aggregate formation can be excluded during the ion annihilation process due to the following reasons: (i) The absence of planar molecular structure. (ii) No remarkable shift between the ECL spectrum and fluorescence spectrum.

(iii) Almost no changes in ECL intensities at different concentrations. (iv) No characteristic peak occurred in fluorescence spectra when the sample concentration is enhanced greatly.

Therefore, the ECL of compounds **C1**–**C3** can be ascribed to the typical and simple monomer ECL emission produced by the annihilation of radical anions and cations during repeated pulsing (Scheme 2). The enthalpy change of the radical ion annihilation reaction $\left(-\Delta H_{ann}^{o}\right)$ is calculated from the following equation:[37]

$$-\Delta H_{ann}^{0}/eV = E_{pa}(1) - E_{pc}(1) - 0.1\,eV \qquad (1)$$

It can be seen from Table 1, the energy $\left(-\Delta H_{ann}^{o}\right)$ provided by the ion-annihilation reaction is larger than that (E_s) required for direct production of the singlet excited state (S-route), and the equation is presented as follows:[37]

$$-\Delta H_{ann}^{0} \geq E_{s} \qquad (2)$$

As a result, in this energy sufficient system, all stable ECL emissions can be observed via S-route without the addition of any co-reactant or additional compound.

Co-reactant ECL

The annihilation ECL mentioned above is generated in a double-potential step by pulsing between the potentials of first oxidation and first reduction of compound. But, the high reduction potentials of **C1**–**C3** are difficult to obtain in many solvents due to the limited solvent windows in our case. Alternatively, ECL can also be generated in a single-potential step (only at the oxidation side) by utilizing TPrA as a co-reactant. Oxidation of TPrA is known to generate a strong reducing agent that reacts with the ECL luminophore to form an excited state and then produce ECL emission (Scheme 3).[1–5]

In this study, the first oxidation potentials of **C1**–**C3** occur at $<$ $+0.7$ V (*vs*. SCE) in 1:1 PhH/MeCN, and that of TPrA peaks at $\sim$

$+0.89$ V in the same manner, both of which are lower than the oxidation potential of the solvent. Under the same experimental conditions, the ECL maxima produced by co-reactant method are the same as that produced by annihilation method. However, the ECL intensities formed in co-reactant reactions are distinctly higher than those formed in annihilation reactions (Fig. 8).

Electrogenerated chemiluminescence (ECL) in water-containing system

The ECL behaviors of compounds **C1**–**C3** have been studied in 4:1 (v/v) MeCN/H_2O mixed solvent. Unfortunately, no matter what method is used, annihilation method or co-reactant method, no any ECL signal is found, which can be ascribed to the following three reasons: (i) The reduction potentials of **C1**–**C3** are beyond that of water, so negative radicals are difficult to be formed and the ECL emissions could not be observed. (ii) The water which is a strong polar solvent could quench the ECL of compounds. (iii) The hydrogen bond between the oxygen atoms in the 15-crown-5 unit and water in the solvent could also make the ECL quench.

CONCLUSION

In conclusion, a series of compounds **C1**–**C3** have been synthesized and the photophysical, electrochemical, and ECL characters in 1:1 PhH/MeCN have been measured. The stable ECL emissions of all compounds can be ascribed to the typical and simple monomer ECL emission via S-route. The ECL intensity is enhanced distinctly with the increase in the fluorescence quantum yield. Under the same experimental conditions, the ECL maxima produced by co-reactant method are the same as that produced by annihilation method. However, the ECL intensities formed in co-reactant reactions are distinctly higher than those formed in annihilation reactions. Although the ECL behaviors of all compounds in water-containing system (4:1 (v/v) MeCN/H_2O) are never found, this study is of vital importance to an understanding of the basic chemistry of the crown ether system and provides evidence for the structure's modification in order to get efficient ECL sensors in the aqueous solution.

EXPERIMENTAL SECTION

Materials and measurements

Anhydrous acetonitrile (chromatographic grade), tetra-*n*-butylammonium hexafluorophosphate (TBAPF$_6$) were obtained from Aldrich and used as received. 4-diphenylamino-benzaldehyde and 2,3,6,7-tetrahydro-1*H*,5*H*-pyrido[3,2,1-*ij*]quinoline-9-carbaldehyde were prepared in-house. Solvents were distilled according to the standard methods and purged with nitrogen before use. *N,N*-Dimethylformamide (DMF) was dried over 4Å molecular sieves and further purified by vacuum distillation over calcined baryta. Tetrahydrofuran (THF) and benzene were purified by distillation over sodium chips and benzophenone under N_2 atmosphere. All other solvents and reagents were of analytical grade quality purchased commercially and used as received unless otherwise stated.

^{1}H NMR spectra were recorded on a VARIAN INOVA 400 MHz NMR instrument (Varian, America) and ^{13}C NMR spectra were

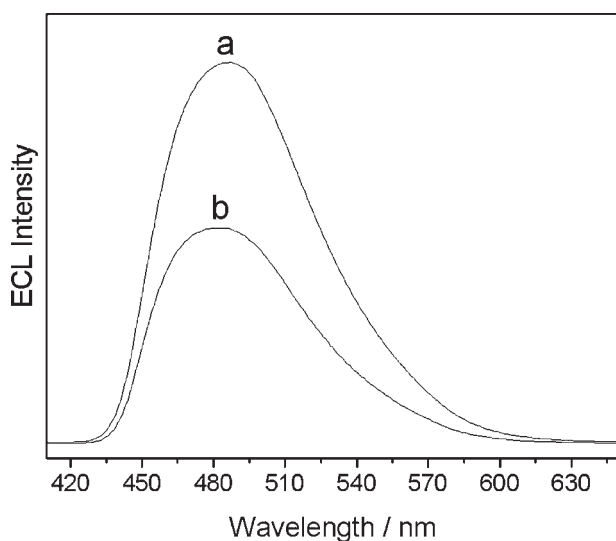**Figure 8.** ECL spectra of the (a) co-reactant reaction and (b) annihilation reaction of 1×10^{-4} M solution of **C3** in 1:1 PhH/MeCN with 0.05 M TBAPF$_6$ as a supporting electrolyte. TPrA (0.01 M) in sample (a), and the potential was stepped from 0 to $+1.0$ V, pulsed for 0.5 s

6

www.interscience.wiley.com/journal/poc

Copyright © 2008 John Wiley & Sons, Ltd.

J. Phys. Org. Chem. **2009**, 22 1–8

recorded on the same instrument at 100 MHz. HRMS were recorded with a GC-TOF mass spectrometry (Micromass, England). All the melting points were not corrected.

All UV–Visible spectra were measured on a HP-8453 spectrophotometer (HP, America) with 1×10^{-5} M solution of the compounds in 1:1 PhH/MeCN solution and all fluorescence spectra on a PTI-C-700 Felix fluorescence spectrophotometer (Hitachi, Japan) using proper solution concentrations in the same solution.

CVs were performed with a BAS-100W Electrochemical Work Station (BAS, America) using a three-electrode conventional electrochemical cell. Measurements were obtained with 1×10^{-3} M solution of the compounds in 1:1 PhH/MeCN solution with 0.05 M TBAPF$_6$. Platinum disk was used as working electrode, platinum wire served as a counter electrode, a Ag/Ag$^+$ electrode was utilized as a reference electrode, and the scan rate was 100 mV s^{-1}. All potentials were calibrated *versus* an aqueous SCE by the addition of ferrocene as an internal standard taking E$^\circ$(Fc/Fc$^+$) = 0.424 V *versus* SCE.[38]

ECL spectra were recorded at room temperature using a setup consisting of a fluorescence spectrophotometer and a cyclic voltammograph with a computer interface. Measurements were obtained with 1×10^{-3} M solution of the compounds in 1:1 PhH/MeCN solution with 0.05 M TBAPF$_6$. In the annihilation reaction, the platinum electrode was pulsed between the first reduction and first oxidation potentials with a pulse width of 0.5 s. In the co-reactant reaction, the platinum electrode was pulsed only on the oxidation side with a pulse width of 0.5 s.

X-ray crystal diffraction data of compounds **C3** were collected at 273 K with a Bruker Smart APEX CCD diffractometer using graphite monochromated Mo-Kα radiation ($\lambda = 0.71073$ Å). The structures were solved by direct methods and subsequent difference Fourier syntheses, and refined by the full-matrix least squares on (F^2) by using the SHELXL-97 program package. The hydrogen atoms were placed in calculated positions and were held riding on their parent non-hydrogen atoms during the subsequent refinement calculations. All non-hydrogen atoms were refined with anisotropic thermal displacement parameters.

Synthetic procedures

1,11-Bis(tosyloxy)-triethylene glycol [Ts(OCH$_2$CH$_2$)$_4$OTs] (1). A solution of tetraethylene glycol (43.3 g, 0.22 mol) and *p*-toluenesulfonyl chloride (127.3 g, 0.67 mol) in THF (500 ml) was placed in a 1 L three-necked round-bottom flask and stirred with a mechanical stirrer. The flask was cooled with an ice–water bath, and a solution of KOH (81.9 g, 1.46 mol) in water (170 ml) was added slowly over a period of 1 h. The ice–water bath was removed, and the system was stirred for an additional 7 h. The resulting suspension was poured into a mixture of CH$_2$Cl$_2$ (200 ml) and ice–water (200 ml), and the aqueous layer was extracted with CH$_2$Cl$_2$. The combined organic solutions were washed three times with distilled water and dried over anhydrous MgSO$_4$ overnight. After removal of MgSO$_4$ and solvent, the oil was purified by silica gel column chromatography (petroleum ether/ethyl acetate 1:2, v/v) to provide the corresponding ditosylate compound **1** (103.1 g, 92%) as colorless oil; ^{1}H NMR (400 MHz, CDCl$_3$), δ (ppm): 7.79 (d, *J* = 8.4 Hz, 4H), 7.34 (d, *J* = 8.0 Hz, 4H), 4.15 (t, *J* = 4.8 Hz, 4H), 3.68 (t, *J* = 4.8 Hz, 4H), 3.55 (s, 8H), 2.44 (s, 6H); HRMS (EI+): C$_{22}$H$_{30}$O$_9$S$_2$, 502.1333 (calculated: 502.1331).

Benzo 15-crown-5 (2). To a stirred solution of catechol (3.3 g, 30 mmol) and Bu$_4$NI (2.8 g (25 mmol%), 7.5 mmol) in toluene (180 ml) 50% NaOH aq (60 ml) at 50–60 °C was added. The mixture was stirred at this temperature for further 30 min, whereupon a solution of ditosylate **1** (15.1 g, 30 mmol) in toluene (180 ml) was added. The resulting mixture was vigorous stirred at reflux for 16 h. The organic layer was separated and washed with H$_2$O (3 × 150 ml), brine (100 ml), and dried over anhydrous MgSO$_4$. The solvent was removed under vacuum to afford a semisolid. Further purification was performed by recrystallization from hexane to afford compound **2** (4.2 g, 52%) as snow flate solid; ^{1}H NMR (400 MHz, CDCl$_3$), δ (ppm): 6.89 (s, 4H), 4.14 (t, *J* = 4.4 Hz, 4H), 3.91 (t, *J* = 4.4 Hz, 4H), 3.77 (s, 8H); HRMS (EI+): C$_{14}$H$_{20}$O$_5$, 268.1313 (calculated: 268.1311).

2,3-(4′,5′-Bis(diethoxyphosphinylmethyl)benzo)-1,4,7,10,13-pentaoxacyclopentadeca-2-ene (4). A 50 ml flask fitted with a reflux condenser was charged with benzo-15-crown-5 (1.01 g, 3.7 mmol), paraformaldehyde (0.44 g, 14.8 mmol) and HOAc (8 ml), HBr in HOAc (5 ml, 40%) was added and the solution was heated on an oil-bath in a well-ventilated fume cupboard at 50 °C overnight. After cooling the solution, the reaction mixture was extracted with CH$_2$Cl$_2$ (3 × 50 ml) and washed with cold water (3 × 50 ml), dried over anhydrous Na$_2$SO$_4$, and the solvent was finally evaporated to afford colorless crystals of **3**. Then, compound **3** was mixed with triethyl phosphite (2.46 g, 14.8 mmol). The viscous solution was stirred at 150 °C overnight. Evaporation of the excess of triethylphosphite, crude product **4** (dark oil) was obtained. This crude product was used without further purification in the next synthesis step.

2,3-{4,5-Bis[(4-dimethylamino-phenyl)-vinyl]-benzo}-1,4,7,10,13-pentaoxacyclopentadeca-2-ene (C1). A suspension of NaH (185 mg (>52% in mineral oil), 4.0 mmol) was thoroughly washed with anhydrous hexane and then suspended in anhydrous THF (8 ml). A solution of **4** (569 mg, 1.0 mmol) in THF (8 ml) was added under nitrogen to this suspension, followed after 10 min by the addition of a solution of 4-*N*,*N*-dimethylamino-benzaldehyde (300 mg, 2.0 mmol) in the same solvent (8 ml). The mixture was cautiously heated on an oil-bath at 50 °C until the evolution of hydrogen had ceased, and then at reflux for 3 h. The mixture was poured into ice water (100 ml) and the aqueous phase was extracted with diethyl ether (4 × 50 ml). The organic phases were combined, washed with water and dried over anhydrous Na$_2$SO$_4$, and the solvent was finally evaporated to afford a dark solid. Further purification was performed by silica gel chromatography (ethyl acetate/hexane 7:2, v/v) to afford compound **C1** (246 mg, 44%) as pale yellow solid; mp: 166–168 °C; ^{1}H NMR (400 MHz, CDCl$_3$), δ (ppm): 7.40 (d, *J* = 8.8 Hz, Hz, 4H), 7.23 (d, *J* = 16.4 Hz, 2H), 7.06 (s, 2H), 6.81 (d, *J* = 16.0 Hz, 2H), 6.32 (d, *J* = 8.4 Hz, 4H), 4.22 (t, *J* = 4.0 Hz, 4H), 3.94 (t, *J* = 4.0 Hz, 4H), 3.78 (s, 8H), 2.98 (s, 12H); ^{13}C NMR (100 MHz, CDCl$_3$), δ (ppm): 150.12, 148.72, 130.05, 129.55, 127.61, 126.56, 122.43, 112.73, 111.81, 71.31, 70.73, 69.84, 69.40, 40.70; HRMS (EI+): C$_{34}$H$_{42}$N$_2$O$_5$, 558.3086 (calculated: 558.3094).

2,3-{4,5-Bis[9-(2,3,6,7-tetrahydro-1*H*,5*H*-Pyrido[3,2,1-*ij*]q-uinoline)-vinyl]-benzo}-1,4,7,10,13-pentaoxacyclo-pentadeca-2-ene (C2). Compound **C2** (4.2 g, 52%) were obtained as brown yellow solid using a similar procedure to **C1**. mp: 177–179 °C; ^{1}H NMR (400 MHz, CDCl$_3$), δ (ppm): 7.12 (d, *J* = 16.0 Hz, 2H), 7.01 (s, 2H), 6.96 (s, 4H), 6.70 (d, *J* = 16.0 Hz, 2H), 4.20 (t, *J* = 4.0 Hz, 4H), 3.92 (t, *J* = 4.0 Hz, 4H), 3.77 (s, 8H), 3.16 (bs, 8H), 2.77 (bs, 8H), 1.99 (m, 8H); ^{13}C NMR (100 MHz, CDCl$_3$), δ (ppm): 148.52, 142.74, 130.29, 129.93, 125.65, 125.48, 121.90, 121.64, 111.97, 71.30,

70.76, 69.87, 69.43, 50.18, 27.87, 22.23; HRMS (EI+): $C_{42}H_{50}N_2O_5$, 662.3719 (calculated: 662.3720).

2,3-{4,5-Bis[(4-diphenylamino-phenyl)-vinyl]-benzo}-1,4,7,10, 13-pentaoxacyclopentadeca-2-ene (C3). Compound **C3** (4.2 g, 52%) were obtained as yellow solid using a similar procedure to **C1**. mp: 109–111 °C; ^1H NMR (400 MHz, CDCl$_3$), δ (ppm): 7.37 (d, $J = 8.4$ Hz, 4H), 7.30 (d, $J = 16.0$ Hz, 2H), 7.27–7.23 (m, 8H), 7.12–7.00 (m, 18H), 6.82 (d, $J = 16.0$ Hz, 2H), 4.22 (t, $J = 3.6$ Hz, 4H), 3.94 (t, $J = 3.6$ Hz, 4H), 3.78 (s, 8H); ^{13}C NMR (100 MHz, CDCl$_3$), δ (ppm): 149.08, 147.70, 147.39, 132.04, 129.80, 129.43, 129.21, 127.43, 124.74, 124.61, 123.80, 123.16, 111.72, 71.26, 70.67, 69.76, 69.30; HRMS (EI+): $C_{54}H_{50}N_2O_5$, 806.3719 (calculated: 806.3720).

SUPPORTING INFORMATION

This paper contains supplememtary information.

Acknowledgements

REFERENCES

[1] M. M. Richter, *Chem. Rev.* **2004**, *104*, 3003–3036. DOI: 10.1021/cr020373d
[2] A. W. Knight, G. M. Greenway, *Analyst* **1994**, *5*, 879–890. DOI: 10.1039/AN9941900879
[3] S. Kulmala, J. Suomi, *Anal. Chim. Acta* **2003**, *500*, 21–69. DOI: 10.1016/j.aca.2003.09.004
[4] A. W. Knight, *Trends Analyt. Chem.* **1999**, *18*(1), 47–62. DOI: 10.1016/S0165-9936(98)00086-7
[5] K. A. Fähnrich, M. Pravda, G. G. Guilbault, *Talanta* **2001**, *54*(4), 531–559. DOI: 10.1016/S0039-9140(01)00312-5
[6] X. B. Yin, B. Qi, X. Sun, X. Yang, E. Wang, *Anal. Chem.* **2005**, *77*(11), 3525–3530. DOI: 10.1021/ac0503198
[7] M. M. Sartin, A. J. Boydston, B. L. Pagenkopf, A. J. Bard, *J. Am. Chem. Soc.* **2006**, *128*(31), 10163–10170. DOI: 10.1021/ja0618494
[8] J. Kim, II, I. S. Shin, H. Kim, J. K. Lee, *J. Am. Chem. Soc.* **2005**, *127*(6), 1614–1615. DOI: 10.1021/ja043721x
[9] C. M. Elliott, F. Pichot, C. J. Bloom, L. S. Rider, *J. Am. Chem. Soc.* **1998**, *120*(27), 6781–6784. DOI: 10.1021/ja974347m
[10] A. M. Anderson, R. Isovitsch, D. Miranda, S. Wadhwa, R. H. Schmehl, *Chem. Commun.* **2000**, 505–506. DOI: 10.1039/a908148h
[11] J. S. Littig, T. A. Nieman, *Anal. Chem.* **1992**, *64*(10), 1140–1144.
[12] R. Y. Lai, *Ph.D. Thesis, the University of Texas at Austin*, 2003; Chapter 1.
[13] X. Yang, X. Jiang, C. Zhao, R. Chen, P. Qin, L. Sun, *Tetrahedron Lett.* **2006**, *47*(28), 4961–4694. DOI: 10.1016/j.tetlet.2006.04.154
[14] X. Jiang, X. Yang, C. Zhao, K. Jin, L. Sun, *J. Phys. Chem. C* **2007**, *111*(26), 9595–9602. DOI: 10.1021/jp071015n
[15] R. Y. Lai, X. Kong, S. A. Jenekhe, A. J. Bard, *J. Am. Chem. Soc.* **2003**, *125*(41), 12631–12639. DOI: 10.1021/ja036600q
[16] I. Prieto, J. Teetsov, M. A. Fox, D. A. V. Bout, A. J. Bard, *J. Phys. Chem. A* **2001**, *105*(3), 520–523. DOI: 10.1021/jp003566i
[17] F. Fungo, K. T. Wong, S. Y. Ku, Y. Y. Hung, A. J. Bard, *J. Phys. Chem. B* **2005**, *109*(9), 3984–3989. DOI: 10.1021/jp045548x
[18] T. I. Ho, A. Elangovan, H. Y. Hsu, S. W. Yang, *J. Phys. Chem. B* **2005**, *109*(18), 8626–8633. DOI: 10.1021/jp0444518
[19] A. Elangovan, K. M. Kao, S. W. Yang, Y. L. Chen, T. I. Ho, Y. O. Su, *J. Org. Chem.* **2005**, *70*(11), 4460–4469. DOI: 10.1021/jo0477953
[20] A. Elangovan, H. H. Chiu, S. W. Yang, T. I. Ho, *Org. Biomol. Chem.* **2004**, *21*, 3113–3118. DOI: 10.1039/B410829A
[21] A. Elangovan, J. H. Lin, S. W. Yang, H. Y. Hsu, T. I. Ho, *J. Org. Chem.* **2004**, *69*(23), 8086–8092. DOI: 10.1021/jo0493424
[22] G. Zhang, D. Zhang, Y. Zhou, D. Zhu, *J. Org. Chem.* **2006**, *71*(10), 3970–3972. DOI: 10.1021/jo052494u
[23] R. E. Gawley, H. Mao, M. M. Haque, J. B. Thorne, J. S. Pharr, *J. Org. Chem.* **2007**, *72*(6), 2187–2191. DOI: 10.1021/jo062506r
[24] S. J. K. Pond, O. Tsutsumi, M. Rumi, O. Kwon, E. Zojer, J. L. Brédas, S. R. Marder, J. W. Perry, *J. Am. Chem. Soc.* **2004**, *126*(30), 9291–9306. DOI: 10.1021/ja049013t
[25] B. D. Muegge, M. M. Richter, *Anal. Chem.* **2002**, *74*(3), 547–550. DOI: 10.1021/ac010872z
[26] R. Y. Lai, M. Chiba, N. Kitamura, A. J. Bard, *Anal. Chem.* **2002**, *74*(3), 551–553. DOI: 10.1021/ac010885c
[27] Y. Chen, G. L. Baker, *J. Org. Chem.* **1999**, *64*(18), 6870–6873. DOI: 10.1021/jo990620m
[28] T. Bogaschenko, S. Basok, C. Kulygina, A. Lyapunov, N. Lukyanenko, *Synthesis* **2002**, 2266–2270. DOI: 10.1055/s-2002-34853.
[29] B. Winkler, A. W. H. Mau, L. Dai, *Phys. Chem. Chem. Phys.* **2000**, (2), 291–295. DOI: 10.1039/a907547j
[30] A. Abbotto, S. Bradamante, A. Facchetti, G. A. Pagani, *J. Org. Chem.* **1997**, *62*(17), 5755–5765. DOI: 10.1021/jo970059x
[31] A. Abbotto, L. Beverina, S. Bradamante, A. Facchetti, C. Klein, G. A. Pagani, M. Redi-Abshiro, R. Wortmann, *Chem. Eur. J.* **2003**, *9*(9), 1991–2007. DOI: 10.1002/chem.200204356
[32] R. A. Velapoldi, H. H. Tønnesen, *J. Fluoresc.* **2004**, *14*, 465–472.
[33] B. Ding, J. Zhang, W. Zhu, X. Zheng, Y. Wu, X. Jiang, Z. Zhang, S. Xu, *Chin. J. Lumin.* **2003**, *24*, 606–611.
[34] J. S. Yang, S. Y. Chiou, K. L. Liau, *J. Am. Chem. Soc.* **2002**, *124*(11), 2518–2527. DOI: 10.1021/ja016416+
[35] P. McCord, A. J. Bard, *J. Electroanal. Chem.* **1991**, *318*, 91–99. DOI: 10.1016/0022-0728(91)85296-2
[36] Crystal structure data for **C3**: $C_{54}H_{50}N_2O_5 \cdot 0.5(C_7H_8)$, $M_r = 851.01$, Triclinic, space group: $P-1$, $a = 13.0034(4)$, $b = 14.4871(5)$, $c = 15.1303(5)$ Å, $\alpha = 113.429(2)°$, $\beta = 103.637(2)°$, $\gamma = 91.994(2)°$, $V = 2515.00(14)$ Å^3, $T = 273(2)$ K, $Z = 2$, $F(000) = 902$, $D_c = 1.124$ g cm^{-3}, $R = 0.1014$, $R_w = 0.2899$ GOF = 1.110. CCDC-642414 contains the supplementary crystallographic data for this paper. These data can be obtained free of charge from the Director, CCDC, 12 Union Road, Cambridge, CB21EZ, UK (Fax: +44-1233-336-033; e-mail: deposit@ccdc.cam.ac.uk or http://www.ccdc.cam.ac.uk).
[37] S. K. Lee, Y. Zu, A. Herrmann, Y. Geerts, K. Müllen, A. J. Bard, *J. Am. Chem. Soc.* **1999**, *121*(14), 3513–3520. DOI: 10.1021/ja984188m
[38] A. Mehlhorn, B. Schwenzer, K. Schwetlick, *Tetrahedron* **1977**, *33*(12), 1489–1491. DOI: 10.1016/0040-4020(77)88010-1